Low-lying octupole isovector excitation in ^{144}Nd

M. Thürauf *et al.*

Low-lying octupole isovector excitation in ^{144}Nd

M. Thürauf,[1] Ch. Stoyanov,[2] M. Scheck,[1,3,4,*] M. Jentschel,[5] C. Bernards,[6] A. Blanc,[5] N. Cooper,[6]
G. De France,[7] E. T. Gregor,[3,4] C. Henrich,[1] S. F. Hicks,[8] J. Jolie,[9] O. Kaleja,[1] U. Köster,[5] T. Kröll,[1]
R. Leguillon,[10] P. Mutti,[5] D. O'Donnell,[3,4] C. M. Petrache,[10] G. S. Simpson,[11] J. F. Smith,[3,4] T. Soldner,[5]
M. Tezgel,[1] W. Urban,[12] J. Vanhoy,[13] M. Werner,[1] V. Werner,[1,6] K. O. Zell,[9] and T. Zerrouki[10]

[1]*Institut für Kernphysik, TU Darmstadt, Schlossgartenstr. 9, 64289 Darmstadt, Germany*
[2]*Institute for Nuclear Research and Nuclear Energy,*
Bulgarian Academy of Sciences, 72 Tzarigradsko Shaussee, 1784 Sofia, Bulgaria
[3]*School of Engineering and Computing, University of the West of Scotland, High Street, Paisley PA1 2BE, UK*
[4]*The Scottish Universities Physics Alliance, University Avenue, Glasgow G12 8QQ, UK*
[5]*Institut Laue-Langevin, 71 avenue des Martyrs, 38000 Grenoble, France*
[6]*Wright Nuclear Structure Laboratory, Yale University,*
P.O. Box 208120, New Haven, CT 06520-8120, USA
[7]*Grand Accélérateur National d'Ions Lourds, Boulevard Henri Becquerel, 14000 Caen, France*
[8]*Dept. of Physics, University of Dallas, Irving, TX 75062, USA*
[9]*Institut für Kernphysik, Universität zu Köln, Zülpicher Str. 77, 50937 Köln, Germany*
[10]*CSNSM, CNRS-IN2P3, Université Paris-Saclay, 91405 Orsay Cedex, France*
[11]*LPSC, UJF Grenoble I, 53 avenue des Martyrs, 38026 Grenoble Cedex, France*
[12]*Faculty of Physics, University of Warsaw, ul. Pasteura 5, 02-093 Warsaw, Poland*
[13]*Department of Physics, U.S. Naval Academy, 121 Blake Road, Annapolis, MD 21402, USA*
(Dated: January 4, 2019)

The nature of low-lying 3^- levels in ^{144}Nd was investigated in the ^{143}Nd(n, $\gamma\gamma$) cold neutron capture reaction. The combination of the high neutron flux from the research reactor at the Institut Laue-Langevin and the high γ-ray detection efficiency of the EXILL setup allowed the recording of $\gamma\gamma$ coincidences. From the coincidence data precise branching ratios were extracted. Furthermore, the octagonal symmetry of the setup allowed angular-distribution measurements to determine multipole-mixing ratios. Additionally, in a second measurement the ultra-high resolution spectrometer GAMS6 was employed to conduct lifetime measurements using the Gamma-Ray Induced Doppler-shift technique (GRID). The confirmed strong $M1$ component in the $3_3^- \rightarrow 3_1^-$ decay strongly supports the assignment of the 3_3^- level at 2779 keV as low-lying isovector octupole excitation. Microscopic calculations within the Quasiparticle Phonon Model confirm an isovector component in the wavefunction of the 3_3^- level, firmly establishing this fundamental mode of nuclear excitation in near-spherical nuclei.

Recently, with the observations of strong $B(E3, 0^+ \rightarrow 3^-)$ reduced transition probabilities for ^{220}Rn, but in particular for ^{224}Ra [1], the nuclear octupole degree of freedom has experienced a renaissance. The observed strong $B(E3)$ value for ^{224}Ra suggests ocupole correlations in the ground state, which are in interplay with the quadrupole deformation predicted to enhance a possible CP-violating nuclear Schiff moment (e.g., see Refs. [2, 3] and references therein). In order to predict this enhancement, and the subsequent gain of sensitivity of experiments using strongly octupole-correlated nuclei in the search for CP violation, a complete understanding of the octupole degree of freedom is mandatory.

At present, for the octupole degree of freedom one of the missing pieces of information is the strength of the isovector coupling constant (ICC) for the proton-neutron part of the octupole-octupole residual interaction. In the nucleus, proton and neutron excitations are distinguished by the isospin degree of freedom. Properties of collective levels with an isovector character, for which in the complex wave function of the collective excitation at least one component of a subsystem is out-of-phase relative to the other components, are very sensitive to the strength of the residual proton-neutron interaction [4, 5]. In the ideal case of equal proton and neutron components, the isoscalar wavefunction is symmetric under the exchange of protons and neutrons, while the isovector wavefunction is antisymmetric. Due to the general attractive nature of the proton-neutron interaction, the isovector level is found at higher energy, while the isoscalar excitation is lowered in energy. The isoscalar excitation, for which all components of the wavefunction are in phase, is usually the lowest-lying state for a given spin and parity. However, in order to reliable fit the ICC, a systematic identification of the isovector levels in several nuclei is mandatory.

Examples of well-established, low-lying isovector excitations are the 1^+ nuclear scissors mode in deformed or the 2^+ quadrupole mixed-symmetry state in near-spherical nuclei. Since its original discovery in 1984 in ^{156}Gd [6], the scissors mode [5] continues to be the subject of intense research efforts in nuclear physics [7, 8]. In near-spherical nuclei, a vast database for low-lying quadrupole isovector excitations exists [5, 9] and various microscopic calculations confirm the isovector nature of these 2^+ levels. In particular, the Quasiparticle
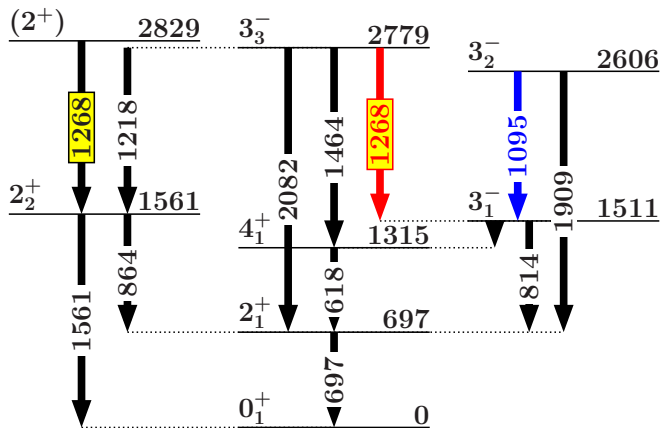
FIG. 1. (Color online) Partial level scheme of low-lying levels in ^{144}Nd. The $3_i^- \to 3_1^-$ transitons are marked in blue ($i = 2$) and red ($i = 3$), respectively. In addition to the decay schemes of the 3_2^- and 3_3^- levels, the 2_i^+ level, from which the second 1268-keV transition originates, is given. This transition obscured the crucial $3_3^- \to 3_1^-$ transition in Ref. [21].

FIG. 2. (Color online) Partial γ-ray spectrum obtained by gating on the 814-keV transision depopulating the 3_1^- level (for a partial level scheme see Fig. 1). The peaks relevant for this work are labeled.

Phonon Model (QPM) [10] has demonstrated its capability to provide an insight into the microscopic structure of levels with a considerable isovector component in their wavefunction (e.g., see Refs. [11–15]). These calculations confirm the sensitivity of the isovector excitation to the residual proton-neutron interaction.

However, for the octupole degree of freedom, only a few candidates for this fundamental excitation mode [16] were proposed [17–19]. Their assignment as a candidate is based on observed strong $M1$ transitions connecting the candidate with the isoscalar state, which is the first excited 3_1^- level. The $M1$ character of the decay to the symmetric state is due to the change of the orbital movement of one subsystem relative to the other subsystem, and the corresponding reduced transition matrix element $\langle 3_{is}^- \| T(M1) \| 3_{iv}^- \rangle$ is expected to be of the order of one nuclear magneton $1\,\mu_N$ [16]. In addition, several candidates exhibit an enhanced $B(E3; 0^+ \to 3_i^-)$ excitation cross section in inelastic particle-scattering experiments [20], which indicates a collective nature. Considering the above mentioned sensitivity of these excitations to the ICC faciliates the necessity to establish firmly this mode in the octupole sector and provide theory with unambiguous experimental data.

A strong candidate for such a low-lying octupole isovector excitation is the 3_3^- level at 2779 keV in the nucleus ^{144}Nd, which is situated only two neutrons above the $N = 82$ shell closure. A partial level scheme containing the levels and transitions relevant to this contribution is shown in Fig. 1. Experimentally, this proposition is based on the previously determined $B(M1, 3_3^- \to 3_1^-) = 0.091^{+52}_{-41}\mu_N^2$ strength [21] and the considerable $E3$ transition strength of $B(E3; 3_3^- \to 0_1^+) = 7.3(7)$ W.u. [22]. In
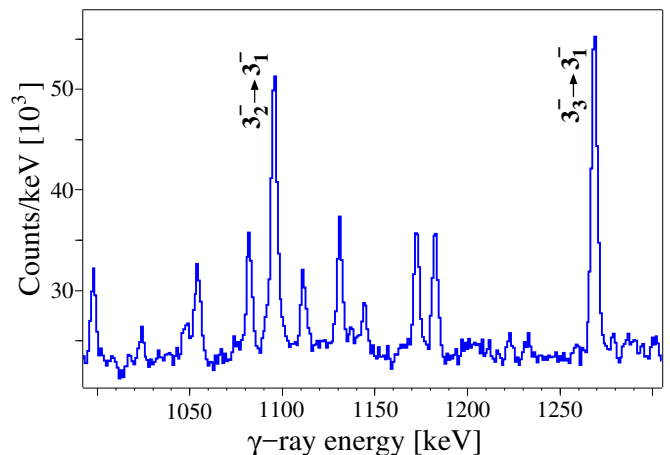
contrast to this state, the 3_2^- state at 2606 keV exhibits a strong $E2$ transition to the 3_1^- level, which is the fingerprint for a quadrupole-octupole coupled $\left[2_1^+ \otimes 3_1^-\right]_{3^-}$ two-phonon state. The strength of $B(E2; 3_2^- \to 3_1^-) = 23(4)$ W.u. [21] is compatible with the $E2$ strength of the $2_2^+ \to 0_1^+$ transition of 17 W.u. In a simplistic vibrational approach, these transitions can be seen as the annihilation of a quadrupole phonon and, therefore, are expected to exhibit the same $E2$ strength. In contrast to the 3_3^- level, which is strongly excited in the inelastic particle scattering, the 3_2^- level is only weakly excited in (p, p') and (d, d') experiments [22] and not excited in (e, e') experiments [23]. These observations point towards a two-phonon nature of the 2606-keV level.

Although the 3_2^- is assigned as the 3^- member of the $\left[2_1^+ \otimes 3_1^-\right]_{J^-}$ quintuplet, a weak $M1$ component is competing with the dominant $E2$ component in the decay to the one-phonon 3_1^- state. In Ref. [21], a $B(M1)$ value of $0.007(1)\,\mu_N^2$ is given for this decay component, which indicates a negligible fragmentation of the $M1$ strength over the 3_2^- and 3_3^- levels due to quantum-mechanical state mixing. Interestingly, in ^{144}Nd, the $2_{1,iv}^+$ state is strongly fragmented over the 2_3^+ and 2_4^+ levels [24].

However, as pointed out in Ref. [21], in the data that were obtained in an $(n, n'\gamma)$ inelastic neutron-scattering experiment, the crucial 1268-keV $3_3^- \to 3_1^-$ transition forms a doublet with a transition from a (2^+) level at 2829 keV to the 2_2^+ level at 1561 keV. Since, this $(n, n'\gamma)$ experiment exclusively used γ-ray singles spectroscopy, it was impossible to disentangle the contributions of the two transitions to the peak. Therefore, the extracted relative γ-ray intensity and multipole-mixing ratio are subject to this ambiguity. However, both experimental quantities are required to determine the $M1$ strength in the $3_3^- \to 3_1^-$ transition, which serves as a benchmark for
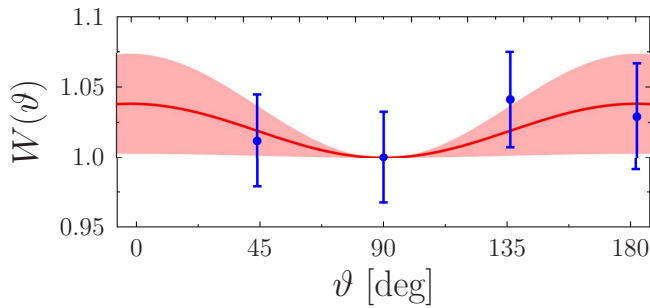
FIG. 3. (Color online) Angular correlation of the 1268-keV $3_3^- \rightarrow 3_1^-$ transition when gated on the 814-keV $3_1^- \rightarrow 2_1^+$ transition.
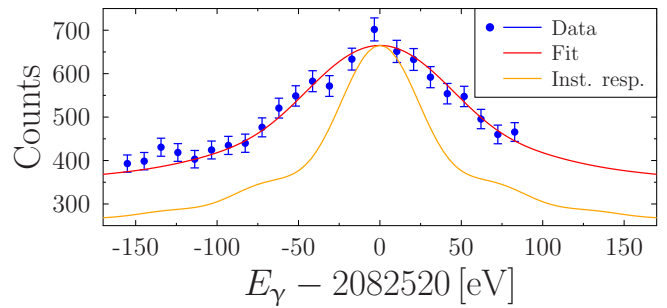

FIG. 4. (Color online) Experimental lineshape (red) of the 2082.52-keV $3_3^- \rightarrow 2_1^+$ transition observed using GAMS6. Additionally, the instrument response curve (yellow) is shown.

theory to explore the nature of the 3_3^- level.

In spite of the experimental indications for the low-lying octupole isovector mode, an investigation of their wavefunctions in a microscopic model such as the QPM is presently lacking. The aim of this work is to provide unambiguous experimental data for the 3_3^- level in ^{144}Nd using $\gamma\gamma$-coincidences recorded in the ^{143}Nd(n,$\gamma\gamma$) reaction and to investigate the wavefunction in the microscopic approach of the QPM.

The cold neutrons were provided by the high-flux research reactor at the Institut Laue-Langevin (ILL) in Grenoble, France, and transported via the PF1B neutron guide to the EXogam at ILL array (EXILL) [25]. At the end of the PF1B neutron guide the neutrons were collimated to a diameter of 12 mm and a flux of 10^8 s^{-1} cm^{-2} was available. The neutrons were impinging on a 0.8 mg target enriched to 91 % in ^{143}Nd. The γ rays emitted following the neutron-capture reaction were detected in the EXILL setup. In this work, the configuration of nine Exogam Clover detectors, five GASP detectors and two ILL Clover detectors was used, which is denoted as Config. 4 in Ref. [25]. The Exogam Clover and GASP detectors were equipped with bismuth germanate active anti-Compton shields.

The data aquisition system operated in triggerless time-stamped mode and every γ-ray event from the detectors was written to the data stream. An offline event-builder was used to identify coincident events. In order to improve the peak-to-background ratio, the eventbuilder contained an add-back algorithm. In 24 hours of beam time a total of 6×10^8 $\gamma\gamma$ coincidences were recorded. An example spectrum recorded using the full array and gated on the 814-keV $3_1^- \rightarrow 2_1^+$ transition is shown in Fig. 2.

The central ring perpendicular to the incident neutrons consisted of eight Exogam Clover detectors, which were mounted in an octagonal symmetry. The four angular groups (45°, 90°, 135°, and 180°) realised in this configuration were used to measure angular correlations of γ-ray cascades, from which, subsequently, the multipole-mixing ratios were extracted.

The $A_2(\delta)$ and $A_4(\delta)$ coefficients in the angular correlation function

$$W(\vartheta) = 1 + Q_2 A_2(\delta) P_2 (\cos \vartheta) + Q_4 A_4(\delta) P_4 (\cos \vartheta) \quad (1)$$

depend on the multipole-mixing ratio δ of the measured transition. The coefficients Q_2 and Q_4 consider the attenuation of the angular distribution due to the finite opening angles of the detectors. They were determined using the well-known transitions of an ^{152}Eu source. For the $3_3^- \rightarrow 3_1^-$ transition, for which the angular correlation function is shown in Fig. 3, a multipole-mixing ratio of $\delta \left(3_3^- \rightarrow 3_1^- \right) = 0.54(4)$ was extracted. In this work the phase convention of Krane, Steffen and Wheeler [26] is used. The branching ratio for this transition was extracted from the $\gamma\gamma$-coincidence data to be $b \left(3_3^- \rightarrow 3_1^- \right) = 35.4(5) \, \%$.

The lifetime $\tau(3_3^-) = 94^{+75}_{-34}$ fs given in Ref. [21] measured with the DSAM-INS technique is also influenced by the 1268-keV doublet in the γ-ray spectra. Therefore, lifetimes were measured with the new instrument GAMS6 using the Gamma-Ray Induced Doppler broadening (GRID) technique [27]. The instrument is a double flat-crystal spectrometer installed at ILL and replaces GAMS4. The main working principle is the same as GAMS4 [28] with the major difference that the entire spectrometer including goniometer axes and interferometers operates under vacuum. This, together with a new optical interferometer layout, optimizes the long-time stability of the angle measurements allowing much longer scans of comparably weak transitions such as the $3_3^- \rightarrow 2_1^+$ 2082-keV transition.

The spectrometer offers two diffraction geometries: i) the non-dispersive, in which both crystals are parallel and ii) the dispersive, in which a dedicated Bragg angle is set in-between the two crystals. In non-dispersive mode the true instrument response function of the spectrometer is determined (see Fig. 4). In dispersive geometry the instrument scans the line profile emitted from the target. Knowing the instrument response allows the association of additional broadening with physical effects in the target.

In the current experiment we used about 12 g of natural Nd_2O_3 powder. The instrument response function was determined from two independent non-dispersive third order measurements of the 618-keV and the 696-keV transitions of ^{144}Nd. The contribution of thermal Doppler broadening was obtained from dispersive third order scans of the same transitions.

The current experiment is the first GRID lifetime measurement carried out with GAMS6, so it was necessary to validate the correctness of extracted lifetimes. This was possible by repeating a former GAMS4 measurement from Ref. [29]. We measured the lifetime of the 3_1^- state using dispersive third order scans of the 814-keV transition. Assuming pure primary feeding a value of $\tau = 1.13_{-14}^{+19}$ ps was obtained. This value agrees well with the upper limit of $0.56 < \tau < 1.21$ ps given in Ref. [29], which corresponds to the same assumptions for the feeding history.

Due to its higher relative intensity $(b(3_3^- \rightarrow 2_1^+) = 39.9(4)\%)$ the $3_3^- \rightarrow 2_1^+$ 2082-keV transition was used to determine the lifetime of the 3_3^- level. The summed result of 13 dispersive first-order scans taken over a time period of five days is shown in Fig. 4. The plot shows a comparison with the instrument response function and clearly exhibits a large Doppler broadening, an indicator for a short lifetime.

In order to extract a lifetime it is mandatory to simulate the motion of the recoiling nucleus. This requires on the one hand the feeding history of the 3_3^- state to be known (this yields the recoil velocity distribution) and on the other hand to model the atomic motion as a function of time after each recoil. We used Molecular Dynamics simulations [30, 31] yielding the most accurate computation description of the atomic motion. The EXILL data allows to estimate the direct feeding from the neutron capture state to be less then 12.5 %. The remaining feeding intensity was taken into account by simulating two-step feeding cascades. Here the energy and the lifetime of the intermediate states are free parameters included in the χ^2 analysis. This procedure results in a lifetime of $\tau_{3_3^-} = 31_{-25}^{+10}$ fs. The complimentary data from both experiments, EXILL and GAMS, allow the calculation of the absolute transition strength as given in Table I. The data confirms the strong M1 component in the $3_3^- \rightarrow 3_1^-$ transition. The error, which is considerable on a relative scale but comparably small on an absolute level, is dominated by the unknown lifetimes of the intermediate levels.

In order to investigate the origin of the observed $M1$ strength, low-lying octupole excitations are explored within the QPM [10]. As already mentioned the model was successfully applied to low-lying quadrupole isovector (mixed-symmetry) states in the domain around the semi-magic number $N = 82$. Following Ref. [10], the main building blocks of the QPM are quasiparticle RPA phonons (QRPA). In the case of even-even nuclei the QPM Hamiltonian is diagonalized in a basis of wavefunctions constructed as a superposition of one-, two-, and three-phonon components [33]. In the present calculation, the parameters of the QPM Hamiltonian are the same as those used in Ref. [14] for ^{144}Nd. The corresponding single-particle spectra for the $A = 144$ region can be found in Refs. [14, 34]. The strengths of the quadrupole-quadrupole and octupole-octupole interactions were fixed according to the properties of the 2_1^+ and 3_1^- levels of ^{144}Nd. The strengths of the other multipole terms are adjusted to keep the energy of the computed two-quasiparticle states unchanged [34]. This set of parameters is widely used and gives an overall description of the low-lying, as well as the high-lying states of nuclei in this mass region [34].

To test the isospin nature of the excited 3^- states, it is useful to compute the ratio [15]

$$\beta(3^-) = \frac{|(M_n - M_p)|^2}{|(M_n + M_p)|^2}, \qquad (2)$$

where

$$M_\tau = \langle 3^- \| \sum_k^\tau r_k^3 Y_{3\mu}(\Omega k) \| g.s. \rangle, \qquad \tau = n, p. \qquad (3)$$

This ratio reveals the dominance of isoscalar correlations $(\beta(3^-) < 1)$ or isovector correlations $(\beta(3^-) > 1)$ in the structure of the excited state.

The first QRPA octupole state is the collective one. The calculated value of the $E3$ transition connecting this state with the ground state is $B(E3; 3_1^- \rightarrow 0_1^+) = 31.3$ W.u. The structure of the $[3_1^-]_{QRPA}$ state reveals that the total contribution of neutrons and protons to the structure of the state is in-phase $(\beta([3_1^-]_{QRPA}) = 0.37)$. The second QRPA octupole state is non-collective and dominated by the proton $1g_{7/2}1h_{11/2}$ two-quasiparticle component. The third QRPA octupole state is slightly collective, and the contribution of the main neutron and proton components in the structure of the state is out-of-phase $(\beta([3_3^-]_{QRPA}) = 2.2)$. This property leads to relatively large value $(B(M1; 3_{3,QRPA}^- \rightarrow 3_{1,QRPA}^-) = 0.36\,\mu_N^2)$ for the $M1$ transition connecting $[3_1^-]_{QRPA}$ and $[3_3^-]_{QRPA}$ states.

The energies and the structure of the low-lying octupole QPM states, which are associated with the observed levels, are given in Table II. The first 3_1^- state is dominated by the isoscalar $[3_1^-]_{QRPA}$ state and, therefore, it is a symmetric state. The second 3_2^- state is mainly a non-collective $[3_2^-]_{QRPA}$ state and in contradiction to the previous statement its two-phonon component is rather small. The third 3_3^- state has a complex structure including 11 % of $[3_3^-]_{QRPA}$ state. The value of Eq. (2) is larger then one $(\beta(3_3^-) = 1.1)$. Therefore, the 3_3^- level has features of the low-lying isovector (mixed-symmetry) state.

TABLE I. Experimental and theoretical reduced transition strengths $B(\sigma L)$ of $3_i^- \to 0_1^+$ and $3_i^- \to 3_1^-$ transitions in ^{144}Nd. E_i and E_γ are given in keV, τ in fs, branching ratios b in %, $B(M1)$ values in units of μ_N^2, and $B(EL)$ values in W.u. For the QPM calculation effective charges of $e_{\rm eff} = 0.1 \cdot e + e_{\rm bare}$ and spin g factors of $g_{\rm s,eff} = 0.8 \cdot g_{\rm s,free}$ were used.

| $J_i \to J_f$ | E_i | E_γ | $\tau(J_i)$ | σL | Exp. – This work | | | QPM | |
					b	δ	$B(\sigma L)$	$E_i^{\rm calc.}$	$B(\sigma L)$
$3_1^- \to 0_1^+$	1511	1511	$^a810^{+110}_{-90}$	$E3$			$^b33.9(17)$	1200	21.0
$3_2^- \to 0_1^+$	2606	2606	$^c153^{+30}_{-16}$	$E3$			$^d1.1(1)$	2820	2.0
$3_2^- \to 3_1^-$		1095		$M1$	18.8(3)	2.0^{+25}_{-8}	0.013(11)		0.04
				$E2$			11^{+5}_{-4}		3.2
$3_3^- \to 0_1^+$	2779	2779	31^{+10}_{-25}	$E3$			$^b7.3(7)$	2904	7.4
$3_3^- \to 3_1^-$		1268		$M1$	35.4(5)	0.54(4)	$0.25^{+1.09}_{-0.08}$		0.17
				$E2$			14^{+70}_{-5}		19.0

[a] Ref. [29]
[b] Ref. [22]
[c] Weighted average from Refs. [21] and [29].
[d] Ref. [32]

TABLE II. Major components of low-lying octupole excitations as determined from QPM calculations.

J_i	Structure
3_1^-	$63\,\%\,[3_1^-]_{\rm QRPA} + 30\,\%\,\left([2_1^+]_{\rm QRPA} \otimes [3_1^-]_{\rm QRPA}\right)$
3_2^-	$66\,\%\,[3_2^-]_{\rm QRPA} + 5\,\%\,\left([2_1^+]_{\rm QRPA} \otimes [3_1^-]_{\rm QRPA}\right)$
3_3^-	$21\,\%\,[3_1^-]_{\rm QRPA} + 11\,\%\,[3_2^-]_{\rm QRPA} + 11\,\%\,[3_3^-]_{\rm QRPA}$ $+32\,\%\,\left([2_1^+]_{\rm QRPA} \otimes [3_1^-]_{\rm QRPA}\right)$

The structure of the low-lying octupole states determines the values of the transition probabilities. In spite the considerable experimental errors, especially for the lifetime of the 3_3^- level, the calculated and measured transitions strengths are, apart from the $B(E2, 3_2^- \to 3_1^-)$ value, in good agreement. Hence, it can be concluded that the observed relatively large $B(M1; 3_3^- \to 3_1^-)$ strength is caused by the isovector correlations in the structure of 3_3^- level, and the sizable value of $E2$ transitions connecting the excited 3_3^- and 3_1^- levels is due to the large contribution of the two-phonon $([2_1^+]_{\rm QRPA} \otimes [3_1^-]_{\rm QRPA})$ component in the structure of the 3_3^- level.

This contribution reports a joint experimental and theoretical investigation of low-lying octupole levels in ^{144}Nd. The work exploited the new opportunity of performing neutron capture experiments with a highly-efficient HPGe detector array and the state-of-the-art GAMS6 spectrometer to resolve experimental ambiguities. These experimental efforts were combined with calculations in the Quasiparticle Phonon Model. The theoretical results confirm the observed $B(M1, 3_3^- \to 3_1^-)$

strength as originating from the isovector contribution in the wavefunction of the 3_3^- level, firmly establishing this fundamental excitation mode in the near-spherical nucleus ^{144}Nd.

[*] Email: marcus.scheck@uws.ac.uk
[1] L. P. Gaffney et al., Nature **497**, 199 (2013).
[2] J. Engel, M. J. Ramsey-Musolf, and U. van Kolck, Prog. Part. Nucl. Phys. **71**, 21 (2013).
[3] J. Dobaczewski, J. Engel, M. Kortelainen, and P. Becker, arXiv:1807.09581v1.
[4] K. Heyde and J. Sau, Phys. Rev. C **33**, 1050 (1986).
[5] K. Heyde, P. von Neumann-Cosel, and A. Richter, Rev. Mod. Phys. **82**, 2365 (2010).
[6] D. Bohle et al., Phys. Lett. B **137**, 27 (1984).
[7] J. Beller et al., Phys. Rev. Lett. **111**, 172501 (2013).
[8] T. Beck et al., Phys. Rev. Lett. **118**, 212502 (2017).
[9] U. Kneissl, N. Pietralla, and A. Zilges, J. Phys. G **32**, R217 (2006).
[10] V. G. Soloviev, *Theory of Atomic Nuclei, Quasiparticles and Phonons* (IOP, London, 1992).
[11] N. Lo Iudice and Ch. Stoyanov, Phys. Rev. C **69**, 044312 (2004).
[12] N. Lo Iudice and Ch. Stoyanov, Phys. Rev. C **62**, 047302

(2000).

[13] N. Lo Iudice and Ch. Stoyanov, Phys. Rev. C **65**, 064304 (2002).

[14] N. Lo Iudice, Ch. Stoyanov, and N. Pietralla, Phys. Rev. C **80**, 024311 (2009).

[15] N. Lo Iudice, V. Yu. Ponomarev, Ch. Stoyanov, A. V. Sushkov, and V. V. Voronov, J. Phys. G: Nucl. **39** 043101 (2012).

[16] N. A. Smirnova et al., Nucl. Phys. A **678**, 235 (2000).

[17] C. Fransen et al., Phys. Rev. C **67**, 024307 (2003).

[18] M. Scheck et al., Phys. Rev. C **81**, 064305 (2010).

[19] A. Hennig et al., Phys. Rev. C **92**, 064317 (2015).

[20] M. Scheck, J. Phys. Conf. Ser. **366**, 012040 (2012).

[21] S. F. Hicks et al., Phys. Rev. C **57**, 2264 (1998).

[22] M. Pignanelli et al., Nucl. Phys. A **559**, 1 (1993).

[23] R. Perrino et al., Nucl. Phys. A **561**, 343 (1993).

[24] N. Pietralla, P. von Brentano, and A. F. Lisetskiy, Prog. Part. Nucl. Phys. **60**, 225 (2008).

[25] M. Jentschel et al., JINST **12**, P11003 (2017).

[26] K. S. Krane, R. M. Steffen, and R. M. Wheeler, Nucl. Data Tables **11**, 351 (1973).

[27] H. G. Börner and J. Jolie, J. Phys. G **217**, 19 (1993).

[28] E. G. Kessler et al., Nucl. Inst. Meth. A **457**, 187 (2001).

[29] S. J. Robinson et al., Phys. Rev. Lett. **73**, 412 (1994).

[30] M. Jentschel et al., Nucl. Inst. Meth. **B114**, 446 (1996).

[31] N. Stritt et al., Phys. Rev. B **59** 6762 (1999).

[32] S. J. Robinson et al., Phys. Lett. B **465**, 61 (1999).

[33] M. Grinberg and Ch. Stoyanov, Nucl. Phys. A **573**, 231 (1994).

[34] S. Galés, Ch. Stoyanov, and A. I. Vdovin, Phys. Rep. **166**, 125 (1988).